Tetragonal Crystalline Carbon Nitrides: Theoretical Predictions

Eunja Kim,[1] Changfeng Chen,[1] Thomas Köhler,[2] Marcus Elstner,[2] and Thomas Frauenheim[2]
[1]*Department of Physics and High Pressure Science Center, University of Nevada, Las Vegas, Nevada 89154*
[2]*Universitaet-GH Paderborn, Fachbereich Physik, Theoretische Physik, 33095 Paderborn, Germany*
(Received 11 August 2000)

New tetragonal phases of crystalline carbon nitride (CN) and their atomic structures have been identified using a self-consistent-charge density-functional tight-binding method. A tetragonal rocksalt structure provides theoretical support to recent experimental evidence for a stoichiometric CN phase with tetragonal symmetry. A body-centered tetragonal CN phase with 1:1 stoichiometry is predicted to be highly stable and of interesting atomic structure with complicated C-C and N-N dimerizations along the c axis. The cubic-to-tetragonal transitions are carefully examined to understand the underlying mechanism.

DOI: 10.1103/PhysRevLett.86.652 PACS numbers: 61.50.Ah, 61.50.Ks, 61.50.Lt, 61.50.Nw

Following the pioneering work by Cohen [1], considerable effort has been devoted to the search and characterization of new carbon nitride (CN) structures theoretically [2–5] and experimentally [6–9]. Beside the α and β-C_3N_4 phases obtained in earlier theoretical work, new stoichiometric CN structures have been proposed by experimental work, such as a fullerenelike [10], a monoclinic [11], and a tetragonal form [12] as well as some other so far unknown phases in CN_x/TiN nanocomposite coatings [13]. Because of the limited quality of the samples, however, the experimental results have resolutions too low to accurately identify the crystal structures. Therefore, theoretical calculations that can provide further details about the atomistic structure, stability, and related physical properties are highly desirable.

In this paper we report a theoretical study of an important class of carbon nitrides, namely, that having the CN(1:1) stoichiometry. These materials have received considerable attention in recent years [12,14–16]. This stoichiometry corresponds to the experimental result [12] showing strong evidence for a new CN phase with tetragonal symmetry. The focus of this work is to search for such new tetragonal CN materials and to study the phase transitions from cubic to tetragonal structures. We have identified the tetragonal rocksalt crystal structure of the newly discovered tetragonal CN phase and also have predicted another stable CN phase with body-centered tetragonal structure yet to be confirmed experimentally. Transitions from cubic to new tetragonal phases are investigated to elucidate the underlying mechanism for the related phase transformations.

For the large-scale total-energy calculations, we use the recently developed self-consistent-charge density-functional based tight-binding (SCC-DFTB) scheme [17–19]. The method is derived from the density-functional theory (DFT) by a second-order expansion of the Kohn-Sham energy functional with respect to charge fluctuations $\delta n(\vec{r})$ relative to a reference density $n_0(\vec{r})$. Efficiently approximating the second-order terms in the density fluctuations by a simple distribution of atom-centered point charges $\Delta q_I = q_I - q_I^0$, estimated within a Mulliken analysis, the second-order Kohn-Sham energy reads

$$E_2^{\mathrm{DFT}} = \sum_i^{\mathrm{occ}} n_i \langle \Psi_i | \hat{H}_0 | \Psi_i \rangle + E_{\mathrm{rep}}[n_0] + \frac{1}{2} \sum_{I,J}^{N} \gamma_{IJ} \Delta q_I \Delta q_J \,. \quad (1)$$

While the first term represents the electronic band structure energy of the system with occupation numbers of single-particle states n_i, E_{rep} as a short-range repulsive two-particle interaction includes the ionic repulsion and the Hartree and exchange-correlation double-counting contributions. Both expressions are determined at the reference density n_0. Finally, the third term explicitly accounts for the long-range interatomic Coulomb interactions between net point charges at different lattice sites and the on-site self-interaction contributions of the single atoms. The interaction integrals γ_{IJ} reduces to the Coulomb form for large distances. They incorporate screening effects for intermediate distances and approximate as on-site terms γ_{II} the chemical hardness or Hubbard parameters of the single atoms.

Representing the single-particle electronic states within a minimal basis linear combination of atomic orbitals expansion $\Psi_i(\vec{r}) = \sum_\nu c_{\nu i} \varphi_\nu(\vec{r} - \vec{R}_I)$ and writing the effective potential $V_{\mathrm{eff}}[n_0(\vec{r})] = V_{\mathrm{ext}} + V_H[n_0] + V_{XC}[n_0]$ in H_0 as a superposition of atomic contributions, the variational minimization of the approximate Kohn-Sham energy $\delta E_2^{\mathrm{DFT}} / \delta \Psi_i^*(\vec{r}) = 0$ with the normalization constraint yields a set of Kohn-Sham equations

$$\sum_\nu^M c_\nu^i (H_{\mu\nu} - \varepsilon_i S_{\mu\nu}) = 0, \quad \forall\ \mu, i \,, \quad (2)$$

which are self-consistent in the Mulliken-charge distribution through the charge modification of the Hamiltonian matrix,

$$H_{\mu\nu} = \langle \varphi_\mu | \hat{H}_0 | \varphi_\nu \rangle + \frac{1}{2} S_{\mu\nu} \sum_K^N (\gamma_{IK} + \gamma_{JK}) \Delta q_K = H_{\mu\nu}^0 + H_{\mu\nu}^1 \quad \forall\ \mu \epsilon I, \nu \epsilon J \,. \quad (3)$$

 0031-9007/01/86(4)/652(4)$15.00

Since we further use a DFT-based two-center construction of Hamiltonian and overlap integrals $H^0_{\mu\nu} = H_{\mu\nu}(n_0)$, $S_{\mu\nu}$ as well as the repulsive interactions $E_{\rm rep}(n_0)$ versus distance [18,19], the SCC-DFTB method combines the simplicity and efficiency of common nonorthogonal two-center tight-binding schemes with a considerably improved accuracy and chemical transferability. The TB parameters for C and N generated using this method have been thoroughly tested on various molecular, amorphous, and crystalline phases involving C and N with excellent results [17–21].

The periodic boundary conditions are applied in all cases during the simulations of the crystal structures. A total of 128 atoms were used for the body-centered tetragonal (BCT) and body-centered cubic (BCC) supercells, and 216 atoms for the zinc blende (ZB), β-tin, and rocksalt supercells. The energetic minimization of the individual structures is obtained at the Γ point ($\vec{k} = 0$) by an optimization of the supercells and subsequent molecular-dynamics annealing simulations of the internal atomic coordinates. To further examine the stability of the tetragonal CN structures, additional variation of the nitrogen content has been considered. We have compared many CN structures in their stability, but in this paper will report on only those related to the cubic-to-tetragonal transitions.

Figure 1 shows the cohesive energy diagram for various CN phases with 1:1 stoichiometry. The calculated equilibrium volume, bulk modulus, and cohesive energy of these CN phases are listed in Table I. All three tetragonal CN phases have lower cohesive energies than those of their counterparts with cubic symmetry. This indicates that tetragonal structures are energetically favorable in crystalline CN with 1:1 stoichiometry. A qualitative understanding of these transitions is obtained by examining the relative strength of bond energies for CN systems [22]. Energetically more favorable bonds are formed when the cubic-to-tetragonal transitions occur in the CN structures considered here.

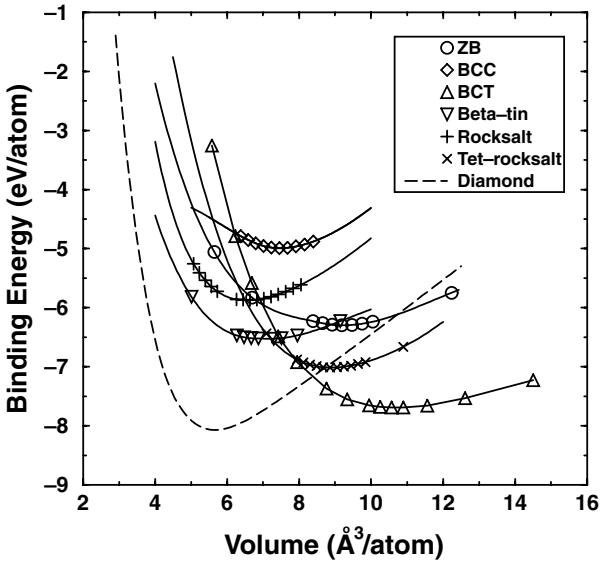

FIG. 1. The cohesive energy diagram of various crystalline CN phases with 1:1 stoichiometry. The result for diamond is also shown for comparison.

Among the considered crystalline structures, we have found that the tetragonal rocksalt phase has structural parameters in excellent agreement with the experimental data [12]. The energy is minimized by compressing the simple cubic rocksalt structure along the c axis and allowing the internal coordinates to be fully relaxed in the a-b plane. This gives an energy gain of 1.14 eV/atom. The calculated lattice constants, a and c, are 5.26 and 2.56 Å, respectively. Although these values are underestimated by about 7% compared to the experimental ones (5.65 and 2.75 Å), the calculated c/a ratio is 0.487, reproducing exactly the experimental value [12]. A charge transfer of $0.1e$ from C to N atoms indicates that weak ionic bonding is superimposed on the strong covalent bonding in this structure. The distance between C atom and the nearest N atom is 1.28 Å, almost the same as the known double bond (C═N) length of 1.29 Å [22].

We further examined two more cubic-to-tetragonal transitions. The first is from the ZB to the β-tin structure. The tetragonal β-tin phase is again found to be more stable than the cubic ZB phase with an energy gain of 0.22 eV/atom. It is interesting to note that the situation is different here from several known cases where cubic structures are more favorable. For example, a pure carbon system favors the cubic diamond phase even under high pressure. In the case of the crystalline silicon and germanium, both prefer the cubic diamond phase rather than the tetragonal β-tin phase, although the latter appears to be stable under high pressure at 10–13 GPa [23].

We next studied the phase transformation from BCC to BCT structure, which turns out to be surprisingly interesting. First of all, the transition is of a much higher energy gain of 2.70 eV/atom, indicating very high stability of the structure. In fact, the cohesive energy of the BCT phase is close to that of diamond (see Table I). The structural optimization of the supercell causes a volume shrinkage from 7.45 Å^3/atom to 6.35 Å^3/atom, resulting in the phase transition from cubic to tetragonal symmetry with a c/a ratio of 0.49 and an energy gain of 1.35 eV/atom. The subsequent molecular dynamics annealing simulations allow further relaxation of the internal atomic positions in the structure. The final structure was obtained by the steepest decent relaxation. Two adjacent N atoms come close to form a N-N dimer with a bond length of 1.12 Å, gaining an additional energy of 0.32 eV/atom. Nitrogen dimers then rotate away from the c axis and form an ordered polymeric chainlike structure (see below), resulting in additional structural and volume changes with a reduced c/a ratio of 0.34 and an extra energy gain of 1.03 eV/atom.

We now discuss more details of the atomic structure of the new BCT phase. Figure 2 shows the fully relaxed BCT structure together with the corresponding BCC structure. We first note that, due to the structural transformation

TABLE I. Calculated equilibrium volume, bulk modulus, and cohesive energy for various CN systems with 1:1 stoichiometry. Results for diamond are also shown for comparison.

	Cohesive energy (eV/atom)	Volume ($Å^3$/atom)	c/a	Bulk modulus (GPa)
ZB	6.30	9.19		192
β-tin	6.52	6.87	0.686	243
BCC	4.99	7.45		332
BCT	7.69	10.9	0.340	243
Rocksalt	5.87	6.63		278
Tet-rocksalt	7.01	8.86	0.487	365
Diamond	8.07	5.67		433

and the subsequent dimerization of N atoms, the distance between N and surrounding C atoms is significantly increased in the BCT phase, yielding a substantially reduced C-N bond strength. Meanwhile, bonds between nearest N atoms become considerably stronger due to the nitrogen dimerization. The N dimers form a polymeric chainlike structure with alternating weak and strong bonds along the c axis, as shown in Fig. 3(a). The N dimer bond lengths of 1.11 and 1.15 Å are close to the value of 1.094 Å for an isolated N_2 molecule [24]. Furthermore, the C atoms that are not bonded with N atoms at the edge of the primitive cell [gray circles in Fig. 2(b)] are again polymerized with alternating bond lengths of 1.16 and 1.52 Å along the c axis, as shown in Fig. 3(b). However, unlike the N dimers that rotate and form a zigzag chain for further energy gain, the C dimers remain along the c axis. Further details on the bonding characters, including the bond angle and bond charge distributions in the BCT phase will be reported elsewhere [21].

It is interesting to note that a polymeric nitrogen chain structure has been proposed in a pure nitrogen phase as the so-called polymeric twofold-coordinated chainlike structure [25]. The structure has the lowest energy among the candidate polymeric phases in the volume regime probed by high-temperature shock compression experiments. An *ab initio* calculation for the pure nitrogen system also suggested that stable nitrogen phases at low temperature under relatively low pressure should be polymeric [26].

Finally, we examined the dependence of the stability of the considered CN phases on the N content in the system. We calculated the cohesive energies of these phases with all possible N contents compatible with the symmetries of these structures. The results are shown in Fig. 4. It is seen that all the considered crystalline CN phases have consistent tendency in cohesive energy that decreases as nitrogen content increases. The tetragonal rocksalt phase remains energetically favorable with consistent energy gain over the rocksalt phase. On the other hand, the β-tin phase becomes nearly degenerate with the ZB phase at 25% and

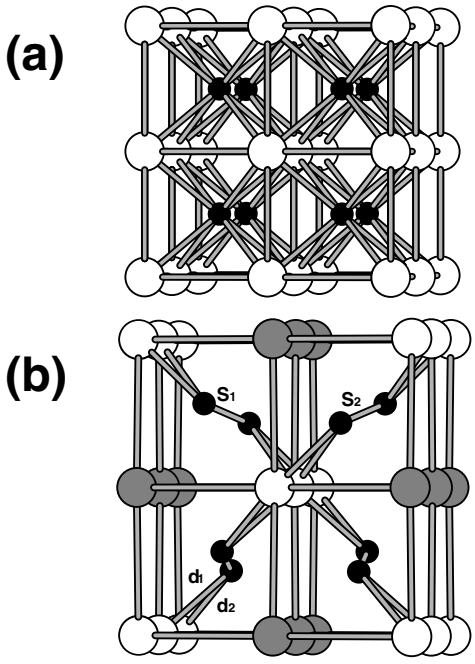

FIG. 2. The fully relaxed geometries of crystalline CN phases with 1:1 stoichiometry. (a) BCC phase. The C-N bond length is 2.15 Å. (b) BCT phase. The black circles represent N atoms, and the gray (open) circles represent C atoms with (without) dimerization along the c axis that points into the paper. The lengths of the two inequivalent C-N bonds are $d_1 = 2.46$ Å and $d_2 = 2.60$ Å; and those for the nitrogen dimers are $S_1 = 1.11$ Å and $S_2 = 1.15$ Å.

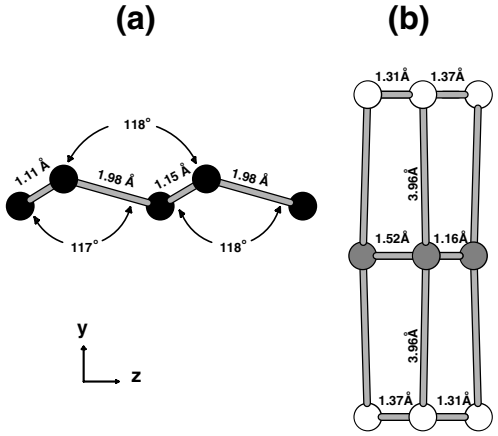

FIG. 3. (a) The zigzag nitrogen polymeric chain structure and (b) the dimerized and undimerized carbon rows along the c axis in the BCT phase of CN with 1:1 stoichiometry. The nearest C-C distance in the a-b plane is 3.96 Å.

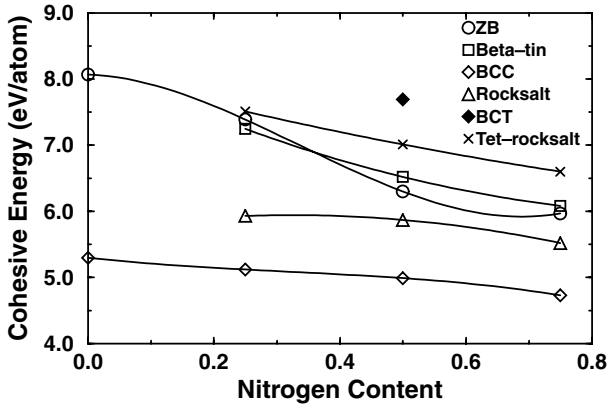

FIG. 4. The cohesive energy of various crystalline CN phases versus the nitrogen content. The BCT phase exists only at 50% N content, i.e., 1:1 stoichiometry in the CN system.

75% N content, whereas at 1:1 stoichiometry the β-tin phase is more stable.

In summary, we have systematically studied the structural stability of various CN phases with 1:1 stoichiometry using the SCC-DFTB method. In particular, we have examined three cubic-to-tetragonal phase transitions: ZB to β-tin, BCC to BCT, and rocksalt to tet-rocksalt. All these transitions have energy gains, indicating that tetragonal symmetry is preferred. We have found that the stability of the tetragonal CN phases are dependent on the N content. The tet-rocksalt phase remains energetically favorable for all considered N contents, while the β-tin phase becomes nearly degenerate with the ZB phase when the N content deviates far from 1:1 stoichiometry. The crystalline CN phase with tetragonal symmetry recently observed in experiment is assigned the tet-rocksalt structure. A new, highly stable BCT phase of crystalline carbon nitride with 1:1 stoichiometry is theoretically predicted and awaits experimental confirmation.

This work was supported by DOE SPS and EPSCoR programs at UNLV and by DFG at Paderborn.

[1] M. L. Cohen, Phys. Rev. B **32**, 7988 (1985).
[2] E. G. Wang, Prog. Mater. Sci. **41**, 242 (1997).
[3] A. Y. Liu and M. L. Cohen, Science **245**, 841 (1989).
[4] A. Y. Liu and R. M. Wentzcovitch, Phys. Rev. B **50**, 10 362 (1994).
[5] D. M. Teter and R. J. Hemley, Science **271**, 53 (1996).
[6] C. Niu, Y. Z. Lu, and C. M. Lieber, Science **261**, 334 (1993).
[7] K. M. Yu, M. L. Cohen, E. E. Haller, W. L. Hansen, A. Y. Liu, and I. C. Wu, Phys. Rev. B **49**, 5034 (1994).
[8] Y. Chen, L. P. Guo, and E. G. Wang, Philos. Mag. Lett. **75**, 155 (1997).
[9] T. Werninghaus, D. R. T. Zahn, E. G. Wang, and Y. Chen, Diam. Relat. Mater. **7**, 52 (1998).
[10] H. Sjöström, S. Stafström, M. Bowman, and J.-E. Sundgren, Phys. Rev. Lett. **75**, 1336 (1995).
[11] L. P. Guo, Y. Chen, E. G. Wang, L. Li, and Z. X. Zhao, Chem. Phys. Lett. **268**, 26 (1997).
[12] L. P. Guo, Y. Chen, E. G. Wang, L. Li, and Z. X. Zhao, J. Cryst. Growth **178**, 639 (1997).
[13] D. Li, X. W. Lin, S. C. Cheng, V. P. Dravid, Y. W. Chung, M. S. Wong, and W. D. Sproul, Appl. Phys. Lett. **68**, 1211 (1996).
[14] M. Cote and M. L. Cohen, Phys. Rev. B **55**, 5684 (1997).
[15] Z. J. Zhang, S. Fan, J. Huang, and C. M. Lieber, J. Electron. Mater. **25**, 57 (1996).
[16] Z. J. Zhang, P. Yang, and C. M. Lieber, Mater. Res. Soc. Symp. Proc. **388**, 271 (1995).
[17] D. Porezag, T. Frauenheim, T. Köhler, G. Seifert, and R. Kaschner, Phys. Rev. B **51**, 12 947 (1995).
[18] M. Elstner, D. Porezag, G. Jungnickel, J. Elsner, M. Haugk, Th. Frauenheim, S. Suhai, and G. Seifert, Phys. Rev. B **58**, 7260 (1998).
[19] T. Frauenheim, G. Seifert, M. Elstner, Z. Hajnal, G. Jungnickel, D. Porezag, S. Suhai, and R. Scholz, Phys. Status Solidi (b) **217**, 41 (2000).
[20] F. Weich, J. Widany, and T. Frauenheim, Phys. Rev. Lett. **78**, 3326 (1997).
[21] E. Kim, C. Chen, T. Köhler, M. Elstner, and T. Frauenheim (unpublished).
[22] I. T. Millar and H. D. Springall, *A Shorter Sidwick's Organic Chemistry of Nitrogen* (Clarendon Press, Oxford, 1969), p. 16.
[23] M. T. Yin and M. L. Cohen, Phys. Rev. B **26**, 5668 (1982).
[24] G. Herzberg, *Spectra of Diatomic Molecules* (B. Van Nosirani, Princeton, 1950), p. 553.
[25] C. Mailhiot, L. H. Yang, and A. K. McMahan, Phys. Rev. B **46**, 14 419 (1992).
[26] D. C. Hamilton and F. H. Ree, J. Chem. Phys. **90**, 4972 (1989).